# $Er^{3+}$-doped tellurofluorophosphate glasses for lasers and optical amplifiers



2005 J. Phys.: Condens. Matter 17 7705

(http://iopscience.iop.org/0953-8984/17/48/020)

INSTITUTE OF PHYSICS PUBLISHING JOURNAL OF PHYSICS: CONDENSED MATTER

J. Phys.: Condens. Matter **17** (2005) 7705–7715 doi:10.1088/0953-8984/17/48/020

# $Er^{3+}$-doped tellurofluorophosphate glasses for lasers and optical amplifiers

**M Jayasimhadri[1], L R Moorthy[1,3], K Kojima[2], K Yamamoto[2], Noriko Wada[2] and Noriyuki Wada[2]**

[1] Department of Physics, Sri Venkateswara University, Tirupati-517502, India
[2] Department of Applied Chemistry, Faculty of Science and Engineering, Ritsumeikan University, Kusatsu, Shiga 525-8577, Japan

E-mail: lrmphysics@yahoo.co.in

Received 18 July 2005, in final form 28 September 2005
Published 11 November 2005
Online at stacks.iop.org/JPhysCM/17/7705

**Abstract**

Absorption, fluorescence and decay properties of erbium-doped alkali tellurofluorophosphate glasses (RTFP) with the molar compositions of 50 $(NaPO_3)_6$–10 $TeO_2$–20 $AlF_3$–19 RF–1 $Er_2O_3$ (R = Li, Na or K) have been investigated in order to utilize these materials for the development of fibre amplifiers and lasers. The Judd–Ofelt (JO) model was applied to the absorption intensities of $Er^{3+}$ ($4f^{11}$) transitions to determine the JO intensity parameters $\Omega_\lambda$ ($\lambda = 2, 4$ or 6). These evaluated intensity parameters are used to calculate the spontaneous emission probabilities and branching ratios from the excited state $J$ manifolds to the lower lying $J'$ manifolds of $Er^{3+}$ emission transitions. The radiative lifetimes of these excited states are determined from their respective spontaneous emission probabilities. Visible and NIR emission spectra have been studied for all three $Er^{3+}$-doped tellurofluorophosphate glasses. In particular, for the emission at 1.5 $\mu$m corresponding to the $^4I_{13/2} \rightarrow {}^4I_{15/2}$ transition, radiative parameters like the full width at half maximum (FWHM), emission cross-sections ($\sigma_e$) and figure of merit (FWHM $\times \sigma_e$) were determined and compared with other hosts. The measured lifetimes of the $^4S_{3/2}$ level are compared with predicted radiative lifetimes calculated from the JO theory. The potentiality of $Er^{3+}$-doped tellurofluorophosphate glasses for devices such as lasers and optical amplifiers is discussed.

## 1. Introduction

In recent years, the incorporation of rare-earth ions into solids has attracted more attention due to potential applications such as planar waveguide amplifiers, short wavelength laser sources, optical amplifiers for telecommunications and solid-state frequency upconverters [1–5].

[3] Author to whom any correspondence should be addressed.

  

$Er^{3+}$-doped glasses are especially attractive for numerous applications such as microchip lasers [6, 7], erbium-doped fibre amplifiers (EDFAs) in wavelength division multiplexing (WDM) systems [8, 9], near infrared telecommunication windows [10], eye safe laser systems [11] and lidar transmitters [12]. In addition, the $Er^{3+}$-doped fluoride fibre laser at 3 $\mu$m radiation acts as a compact and efficient source for applications in medical and micro-surgery [13, 14]. In the current trend, wavelength division multiplexing systems require amplifier materials with increased transmission capacity in order to obtain broader gain bandwidth for the development of computer networks and other data transmitting services. A wide bandwidth optical amplifier is vital for the development of multichannel transmission systems. The amplification bandwidth of the conventional $SiO_2$-based EDFA is limited [15, 16]. Host glasses based on tellurium oxide doped by $Er^{3+}$ ions exhibit large stimulated emission cross-section and broader fluorescence half-width at 1.5 $\mu$m [17]. The low phonon energies of these glasses reduce the non-radiative transition rates of the rare-earth ions when compared to silica and borate glasses [18]. Moreover, wide infrared transmittance, good chemical durability and also the large refractive index values influence the emission cross-sections of rare-earth ion transitions in tellurite-based glasses [15, 19]. With the addition of fluorides into the tellurite-based rare-earth-doped glasses, one can obtain broad amplifier bandwidth with an intrinsically flat gain required for the development of optical transmission networks [20]. These special optical properties as well as their potential applications motivated us to undertake the present study.

In the present work, a Judd–Ofelt (JO) analysis [21, 22] for the absorption bands of $Er^{3+}$ ions in tellurofluorophosphate glass host was performed in order to determine the optical intensity parameters, spontaneous emission probabilities, branching ratios and radiative lifetimes for various excited manifold-to-manifold transitions. Furthermore, complete knowledge of various radiative spectroscopic properties is essential in order to design and develop optical glass materials for device applications. From the fluorescence spectra, the emission cross-sections, bandwidths and lifetimes for certain luminescent levels of $Er^{3+}$ in tellurofluorophosphate glasses are estimated. In particular, the fluorescence properties of the $^4I_{13/2} \rightarrow {}^4I_{15/2}$ transition located around 1534 nm are discussed. The measured lifetimes and non-radiative relaxation rates are also reported for the excited $^4S_{3/2}$ level in all the tellurofluorophosphate glasses.

## 2. Experimental procedure

The alkali tellurofluorophosphate (RTFP) glasses used in the present study were prepared by doping 1 mol% of Er with the chemical compositions of 50 $(NaPO_3)_6$–10 $TeO_2$–20 $AlF_3$–19 LiF–1 $Er_2O_3$ (LiTFP); 50 $(NaPO_3)_6$–10 $TeO_2$–20 $AlF_3$–19 NaF–1 $Er_2O_3$ (NaTFP); and 50 $(NaPO_3)_6$–10 $TeO_2$–20 $AlF_3$–19 KF–1 $Er_2O_3$ (KTFP). Batches of 10 g starting materials of $Er_2O_3$, $(NaPO_3)_6$, $TeO_2$, $AlF_3$ and RF (R = Li, Na and K) were fully mixed and melted in a platinum crucible at 960 °C for 30 min in an electrical furnace. Then the melt was poured into a preheated brass mould and annealed for 10 h at a temperature close to the softening point of the glasses (350 °C). These samples were polished to flat and parallel faces for optical measurements. The refractive indices were measured on an Abbe refractometer by using the sodium lamp as the light source. The density measurements were made by the Archimedes method with water as the immersion liquid. The $Er^{3+}$ concentrations were calculated from the initial glass composition and the sample densities. The refractive indices, densities and the $Er^{3+}$ concentrations of the three glass samples are shown in table 1.

Electronic absorption spectra were recorded with a Varian Cary 5E UV–VIS–NIR spectrophotometer over a spectral range of 340–1650 nm. The visible fluorescence spectra in

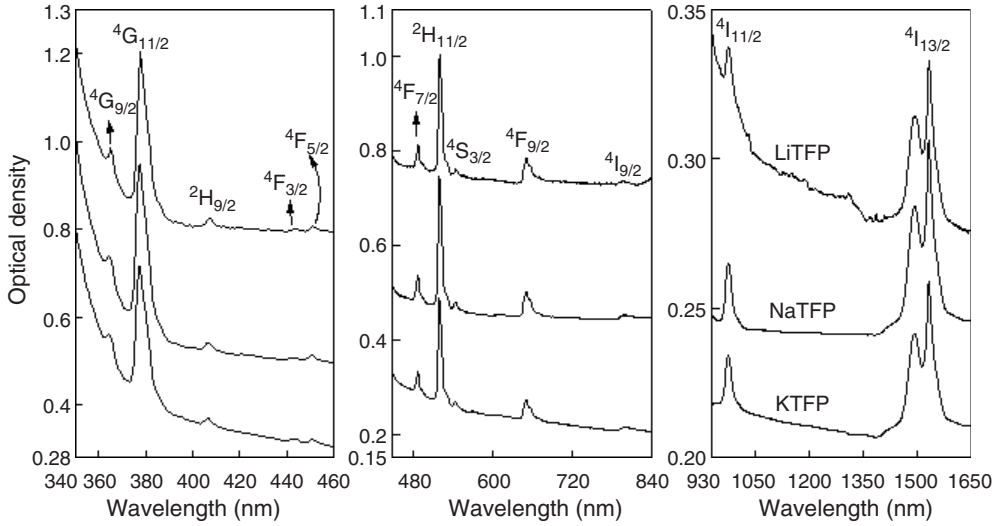


**Figure 1.** UV–VIS–NIR absorption spectra of $Er^{3+}$-doped RTFP glasses.

**Table 1.** Measured physical properties for $Er^{3+}$:RTFP glasses.

| Physical quantities | LiTFP | NaTFP | KTFP |
|---|---|---|---|
| Sample thickness (mm) | 2.50 | 2.37 | 2.26 |
| Refractive index | 1.585 | 1.586 | 1.582 |
| Density (g $cm^{-3}$) | 2.62 | 2.62 | 2.60 |
| Concentration (mol $l^{-1}$) | 0.151 | 0.150 | 0.147 |
| Concentration (ions $cm^{-3} \times 10^{20}$) | 0.907 | 0.902 | 0.885 |

the range 500–700 nm were measured with a Hitachi F-3010 fluorescence spectrophotometer by exciting the samples at 380 nm, using a xenon lamp as an excitation source. The near-infrared fluorescence spectra in the wavelength range 1400–1700 nm were measured by using a computer controlled 970 nm diode laser (SDL-6362-P1) as an excitation source, InGaAs photo diode detector, lock-in-amplifier (Li-570A) and monochromator (Ni Kon G-250). Room-temperature decay lifetimes for the $^4S_{3/2}$ level were measured with a pulsed tunable laser (Lambda Physics, Scan Mate OPPO) under 540 nm excitation by monitoring the emission at 546 nm, and the signal was collected by using a digital oscilloscope (Le Croy LS 140 100 Mz).

## 3. Results and discussion

### *3.1. Absorption spectra and Judd–Ofelt analysis*

The recorded optical absorption spectra of $Er^{3+}$-doped alkali tellurofluorophosphate glasses are shown in figure 1. A total of 12 absorption bands are identified and the assignment of the transitions from the ground state $^4I_{15/2}$ to various excited states are indicated. The most intense absorption bands at 378 and 520 nm are attributed to the $^4I_{15/2} \rightarrow {}^4G_{11/2}$ and $^4I_{15/2} \rightarrow {}^2H_{11/2}$ hypersensitive transitions, respectively [23].

The experimental oscillator strengths $f_{\exp}$ can be determined form the room-temperature absorption spectra by [24]

$$f_{\exp} = \frac{mc^2}{N\pi e^2} \int \varepsilon(\upsilon)\, \mathrm{d}\upsilon \tag{1}$$

where the term before the integral is represented by atomic constants ($m$ and $e$ are the mass and charge of the electron, $c$ is the velocity of light). The integral itself corresponds to the area under the absorption curve. $\varepsilon(\upsilon)$ is the molar absorption coefficient and $f$ is a dimensionless quantity. These $f_{\text{exp}}$ values have been used to determine the JO intensity parameters $\Omega_\lambda$ by a least squares fit. According to the JO theory [21, 22], the calculated oscillator strengths from the initial state to an excited state are

$$f_{JJ'} = \frac{8\pi^2 mc\upsilon}{3he^2(2J+1)}[\chi S_{\text{ed}}(JJ') + nS_{\text{md}}(JJ')] \tag{2}$$

where $\chi = \frac{(n^2+2)^2}{9n}$ is a factor for the effective field at a well-localized centre in a medium with an isotropic refractive index and $S_{\text{ed}}$ and $S_{\text{md}}$ are the electric and the magnetic dipole line strengths which are given by

$$S_{\text{ed}}(JJ') = e^2 \Sigma \Omega_\lambda (\psi J||U^\lambda||\psi' J') \tag{3}$$

$$S_{\text{md}}(JJ') = \left(\frac{e\hbar}{4\pi mc}\right)(\psi J||L+2S||\psi' J')^2 \tag{4}$$

where $||U^\lambda||$ are the double reduced matrix elements of the unit tensor operator of rank $\lambda = 2, 4, 6$ calculated from the intermediate coupling approximation [25]. In our JO analysis we have utilized the reduced matrix elements reported by Ravi Kanth Kumar *et al* [26], since these matrix elements depend only on the rare-earth ion and not on the host material. A measure of the accuracy of the fit between the experimental and calculated oscillator strengths is given by the root mean square (rms) deviation

$$\sigma_{\text{rms}} = \left[\frac{\Sigma(f_{\text{exp}} - f_{\text{cal}})^2}{N}\right]^{1/2} \tag{5}$$

where $N$ is the number of levels included in the fit. The small rms deviations of $\pm 0.299$, $\pm 0.224$ and $\pm 0.247$ ($\times 10^{-6}$) shown in table 2 indicate good fit between the experimental and calculated oscillator strengths. However the effect of the host on the JO parameters influences the radiative transition probabilities, since they contain the crystal-field parameters, inter-configurational radial integrals and the interaction between the central ion and the environment [27]. In table 3, the magnitudes of the three JO intensity parameters evaluated in the present work increase in the order $\Omega_2 > \Omega_4 > \Omega_6$ and are comparable with other reported values for different hosts [27–30]. Generally, the $\Omega_2$ parameter is sensitive to the symmetry of the rare-earth site and is strongly affected by covalency between rare-earth ions and ligand anions, whereas $\Omega_4$ and $\Omega_6$ are related to the rigidity of the host medium in which the ions are situated [31]. In the present work, the $\Omega_2$ values are larger than that of $Er^{3+}$-doped fluorophosphate [23], YAG [28], silicate and fluoride [32] host materials, which indicates that $Er^{3+}$-doped tellurofluorophosphate glasses are more covalent in character, with higher symmetry. The spectroscopic quality factor ($X = \Omega_4/\Omega_6$) [33] values determined for $Er^{3+}$ in LiTFP, NaTFP and KTFP are found to be 0.934, 0.743 and 0.477 respectively, which are within the range of 0.5–1.0 for $Er^{3+}$ ions in different hosts [27–30].

The magnetic dipole line strength ($S_{\text{md}}$) exists only for certain transitions between the states which obey the transition selective rules $\Delta S = \Delta L = 0$, $\Delta J = 0, \pm 1$ [21, 22]. In order to obtain broadband and flat 1.5 $\mu$m emission spectra, it is more essential to increase the relative contribution of the electric dipole transition ($S_{\text{ed}}$) [24]. But, $S_{\text{md}}$ is independent of the ligand fields and is a characteristic of the particular transition determined by the quantum numbers, whereas $S_{\text{ed}}$ is a function of glass structure and composition and can be calculated according to equation (3), by using JO theory. However, it is possible to increase the electric dipole contribution ($S_{\text{ed}}$) by modifying the composition and the structure of the host glass. The

**Table 2.** Experimental ($f_{exp}$) and calculated ($f_{cal}$) oscillator strengths ($\times 10^{-6}$) for the absorption bands of $Er^{3+}$ in RTFP glasses.

| Transition | LiTFP | | | NaTFP | | | KTFP | | |
|---|---|---|---|---|---|---|---|---|---|
| $^4I_{15/2} \rightarrow$ | Energy | $f_{exp}$ | $f_{cal}$ | Energy | $f_{exp}$ | $f_{cal}$ | Energy | $f_{exp}$ | $f_{cal}$ |
| $^4I_{13/2}$ | 6 517 | 1.4892 | 1.3183 | 6 517 | 1.5868 | 1.4550 | 6 517 | 1.5804 | 1.4232 |
| $^4I_{11/2}$ | 10 233 | 0.2658 | 0.6346 | 10 243 | 0.5445 | 0.7258 | 10 243 | 0.5173 | 0.7054 |
| $^4I_{9/2}$ | 12 559 | 0.1502 | 0.2448 | 12 528 | 0.2814 | 0.2186 | 12 512 | 0.3841 | 0.1456 |
| $^4F_{9/2}$ | 15 333 | 2.0065 | 1.8787 | 15 357 | 1.8793 | 1.8674 | 15 357 | 1.4791 | 1.5621 |
| $^4S_{3/2}$ | 18 344 | 0.2747 | 0.5120 | 18 377 | 0.3016 | 0.5707 | 18 377 | 0.2875 | 0.5736 |
| $^2H_{11/2}$ | 19 189 | 7.0682 | 7.3971 | 19 226 | 8.7936 | 8.9613 | 19 226 | 7.6577 | 7.5408 |
| $^4F_{7/2}$ | 20 486 | 1.4308 | 1.9634 | 20 486 | 1.7379 | 2.1043 | 20 486 | 1.5114 | 2.0034 |
| $^4F_{5/2}$ | 22 167 | 0.3451 | 0.6176 | 22 167 | 0.3155 | 0.6872 | 22 167 | 0.3761 | 0.6907 |
| $^4F_{3/2}$ | 22 516 | 0.1790 | 0.3545 | 22 567 | 0.1515 | 0.3953 | 22 567 | 0.1171 | 0.3973 |
| $^2H_{9/2}$ | 24 563 | 0.4130 | 0.7315 | 24 624 | 0.5245 | 0.7999 | 24 563 | 0.5239 | 0.7798 |
| $^4G_{11/2}$ | 26 448 | 13.3940 | 13.0256 | 26 448 | 15.9365 | 15.7534 | 26 448 | 13.1320 | 13.2567 |
| $^4G_{9/2}$ | 27 390 | 0.9177 | 1.2199 | 27 465 | 1.1034 | 1.1894 | 27 465 | 1.0584 | 0.9568 |
| rms ($\times 10^{-6}$) | | ±0.299 | | | ±0.224 | | | ±0.247 | |

**Table 3.** A comparison of evaluated Judd–Ofelt intensity parameters $\Omega_\lambda$ ($10^{-20}$ $cm^2$) of $Er^{3+}$ in different hosts.

| Glass | $\Omega_2$ | $\Omega_4$ | $\Omega_6$ | Order | $\Omega_4/\Omega_6$ | Reference |
|---|---|---|---|---|---|---|
| LiTFP | 4.697 | 1.210 | 1.296 | $\Omega_2 > \Omega_6 > \Omega_4$ | 0.934 | This work |
| NaTFP | 5.918 | 1.070 | 1.441 | $\Omega_2 > \Omega_6 > \Omega_4$ | 0.743 | This work |
| KTFP | 5.086 | 0.693 | 1.453 | $\Omega_2 > \Omega_6 > \Omega_4$ | 0.477 | This work |
| Phosphate | 6.280 | 1.030 | 1.390 | $\Omega_2 > \Omega_6 > \Omega_4$ | 0.740 | [27] |
| YSGG | 0.920 | 0.480 | 0.870 | $\Omega_2 > \Omega_6 > \Omega_4$ | 0.550 | [28] |
| LSS | 7.610 | 1.850 | 2.090 | $\Omega_2 > \Omega_6 > \Omega_4$ | 0.880 | [29] |
| PSS | 4.990 | 1.510 | 2.320 | $\Omega_2 > \Omega_6 > \Omega_4$ | 0.650 | [29] |
| CaLiBO | 3.680 | 0.760 | 1.520 | $\Omega_2 > \Omega_6 > \Omega_4$ | 0.500 | [30] |

calculated line strength ratios of $S_{ed}/(S_{ed}+S_{md})$ for the $^4I_{13/2} \rightarrow {}^4I_{15/2}$ transition of $Er^{3+}$-doped LiTFP (0.752), NaTFP (0.769) and KTFP (0.766) glasses are found to be larger than those of fluoride (0.683), silicate (0.675), phosphate (0.652), germanate (0.568) glasses [34, 35], thereby indicating that $Er^{3+}$:RTFP glasses are more preferable for device applications.

The JO intensity parameters presented in table 3 are used to estimate the radiative transition probabilities between an excited state ($J$) and the lower-lying terminal levels ($J'$) using the following expression:

$$A_R(J, J') = \frac{64\pi^4 v^3}{3h(2J+1)}\left[\frac{n(n^2+2)^2}{9}S_{ed} + n^3 S_{md}\right]. \quad (6)$$

The total radiative transition probability $A_T(J) = \Sigma_{J'} A_R(J, J')$ of any excited state can be obtained by adding the radiative transition probabilities $A_R(J, J')$ calculated for all the terminal states. The radiative lifetimes $\tau_R$ of an excited state ($J$) can be extracted from the total radiative transition probability using the expression

$$\tau_R(J) = \frac{1}{\Sigma_{J'} A_R(J, J')} = [A_T(J)]^{-1}. \quad (7)$$

The predicted radiative lifetimes for various excited luminescent levels of $Er^{3+}$:RTFP glasses shown in table 4 are comparable with those obtained in other different hosts [27, 30, 36].

**Table 4.** Comparison of predicted radiative lifetimes ($\tau_R$) for various excited levels of $Er^{3+}$:RTFP glasses with different hosts.

| Excited states | LiTFP ($\mu$s) | NaTFP ($\mu$s) | KTFP ($\mu$s) | Phosphate ($\mu$s) [27] | LiBO ($\mu$s) [30] | GPTC ($\mu$s) [36] |
|---|---|---|---|---|---|---|
| $^4G_{11/2}$ | 43 | 36 | 43 | — | 78 | — |
| $^2H_{9/2}$ | 319 | 283 | 309 | — | — | — |
| $^4F_{5/2}$ | 362 | 337 | 357 | — | 686 | — |
| $^4F_{7/2}$ | 288 | 275 | 301 | 290 | 534 | — |
| $^2H_{11/2}$ | 153 | 127 | 151 | 120 | — | 67 |
| $^4S_{3/2}$ | 575 | 513 | 514 | 560 | 1 111 | 340 |
| $^4F_{9/2}$ | 753 | 747 | 888 | 880 | 1 333 | 364 |
| $^4I_{9/2}$ | 6076 | 6340 | 8046 | 7780 | 10 694 | 3150 |
| $^4I_{11/2}$ | 5565 | 4896 | 5070 | 6140 | 10 342 | 3300 |
| $^4I_{13/2}$ | 6836 | 6345 | 6488 | 9960 | 11 320 | 3640 |

In all three glasses the radiative lifetimes of the excited states decreases in the order $^4I_{13/2} > {}^4I_{9/2} > {}^4I_{11/2} > {}^4F_{9/2} > {}^4S_{3/2} > {}^4F_{5/2} > {}^2H_{9/2} > {}^4F_{7/2} > {}^2H_{11/2} > {}^4G_{11/2}$ with an exception of the $^4I_{9/2}$ level in the KTFP glass sample. This may be due to the decrease of $\Omega_4$ in KTFP glass, when compared with LiTFP and NaTFP glasses. The fluorescence branching ratios $\beta_R$ from the relaxation state ($J$) to a particular final level ($J'$) can be determined from the radiative decay rates by

$$\beta_R(J, J') = \frac{A_R(\psi J; \psi' J')}{A_T(J, J')} = A_R(J, J')\tau_R. \tag{8}$$

The fluorescence branching ratio is a critical parameter for the laser designer, because it characterizes the possibility of attaining stimulated emission on any specific transition.

### *3.2. Visible fluorescence spectra*

The partial level energy diagram of $Er^{3+}$ in tellurofluorophosphate glasses is shown figure 2, with visible and near-infrared emissions indicated by dotted and solid lines. The visible fluorescence spectra of $Er^{3+}$-doped tellurofluorophosphate glasses are shown in figure 3. Four emission transitions $^2H_{11/2} \rightarrow {}^4I_{15/2}$, $^4S_{3/2} \rightarrow {}^4I_{15/2}$, $^4F_{5/2} \rightarrow {}^4I_{13/2}$, and $^4F_{9/2} \rightarrow {}^4I_{15/2}$, centred nearly at 520, 550, 625 and 674 nm respectively, are detected for $Er^{3+}$:RTFP glasses upon 380 nm excitation. The peak stimulated emission cross-section $\sigma_e(\lambda_P)$, which is essential in predicting the performance of lasing action, can be determined from the following expression:

$$\sigma_e(\lambda_P) = \frac{\lambda_P^4}{8\pi c n^2 \Delta\lambda_{eff}} A_R(J, J') \tag{9}$$

where $\lambda_P$ is the peak wavelength and $\Delta\lambda_{eff}$ is the effective linewidth of the emission band. From table 5, it is observed that the two emission levels corresponding to $^2H_{11/2} \rightarrow {}^4I_{15/2}$ and $^4F_{9/2} \rightarrow {}^4I_{15/2}$ transitions possess large emission cross-sections and high branching ratios, thereby suggesting that these transitions have the most potential for visible laser emission.

### *3.3. NIR fluorescence spectra*

The near-infrared fluorescence spectra of $Er^{3+}$-doped RTFP glasses measured at 1.5 $\mu$m corresponding to the $^4I_{13/2} \rightarrow {}^4I_{15/2}$ transition upon 970 nm laser excitation are shown in

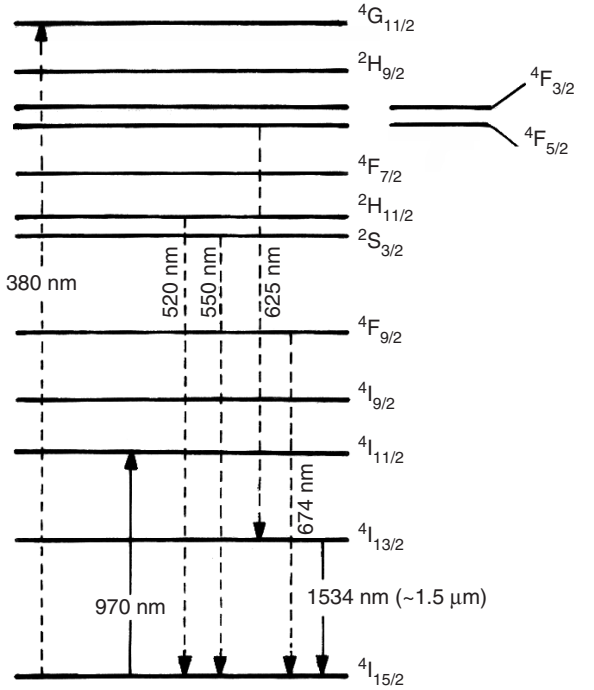


**Figure 2.** Partial energy level diagram showing visible and near-infrared emissions in $Er^{3+}$-doped tellurofluorophosphate glasses.

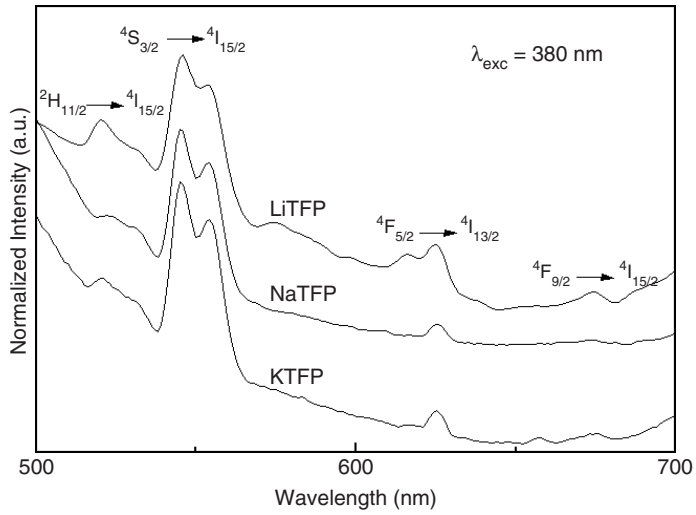


**Figure 3.** UV-excited visible fluorescence spectra of $Er^{3+}$-doped RTFP glasses.

figure 4. The 970 nm laser excitation wavelength corresponds to the $^4I_{11/2} \leftarrow {}^4I_{15/2}$ state, which in turn non-radiatively relaxes to $^4I_{13/2}$. From this state, only the radiative emission to the $^4I_{15/2}$ ground state is possible, since the energy gap is nearly ~6500 $cm^{-1}$. The peak emission wavelengths, radiative transition rates, stimulated emission cross-sections ($\sigma_e$) and

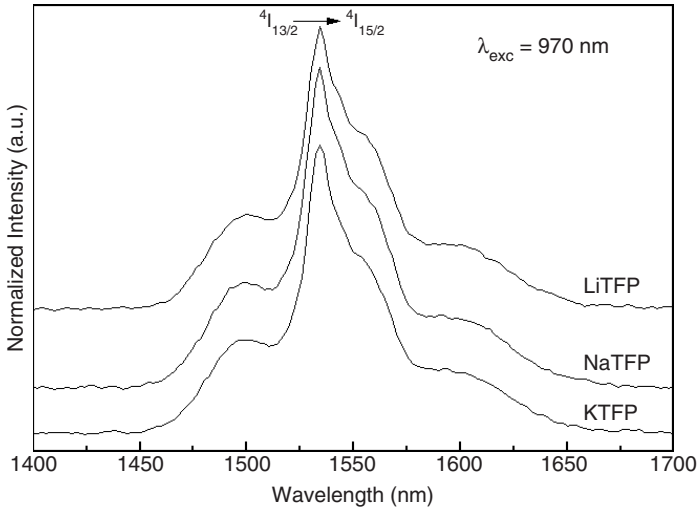


**Figure 4.** Near-infrared fluorescence spectra of the $^4I_{13/2} \rightarrow {}^4I_{15/2}$ transition centred at 1534 nm in $Er^{3+}$-doped tellurofluorophosphate glasses under 970 nm excitation.

**Table 5.** Emission peak wavelengths ($\lambda_P$ nm), radiative transition probabilities ($A$, $s^{-1}$), stimulated emission cross-sections ($\sigma_e \times 10^{-22}$) and branching ratios ($\beta$) for $Er^{3+}$:RTFP glasses.

| | | LiTFP | | | NaTFP | | | KTFP | | |
|---|---|---|---|---|---|---|---|---|---|---|
| Level | $\lambda_P$ | $A$ | $\sigma_e$ | $\beta_{cal}$ | $A$ | $\sigma_e$ | $\beta_{cal}$ | $A$ | $\sigma_e$ | $\beta_{cal}$ |
| $^2H_{11/2} \rightarrow {}^4I_{15/2}$ | 520 | 6085.20 | 345.63 | 0.933 | 7409.86 | 426.87 | 0.939 | 6203.82 | 450.12 | 0.935 |
| $^4S_{3/2} \rightarrow {}^4I_{15/2}$ | 550 | 1169.13 | 34.09 | 0.673 | 1309.52 | 40.53 | 0.673 | 1309.54 | 40.88 | 0.674 |
| $^4F_{5/2} \rightarrow {}^4I_{13/2}$ | 625 | 1094.27 | 100.88 | 0.400 | 1137.17 | 188.50 | 0.384 | 1023.73 | 142.90 | 0.366 |
| $^4F_{9/2} \rightarrow {}^4I_{15/2}$ | 674 | 1184.92 | 166.20 | 0.893 | 1183.34 | 219.75 | 0.884 | 985.39 | 158.56 | 0.876 |
| $^4I_{13/2} \rightarrow {}^4I_{15/2}$ | 1534 | 146.27 | 112.92 | 1.000 | 157.59 | 117.02 | 1.000 | 154.12 | 124.21 | 1.000 |

radiative branching ratios ($\beta_R$) for the $^4I_{13/2} \rightarrow {}^4I_{15/2}$ near-infrared emission of $Er^{3+}$-doped tellurofluorophosphate glasses are also included in table 5. On combining equations (6) and (9), one can observe that the stimulated emission cross-section ($\sigma_e$) is directly proportional to the refractive index of the glass host ($\sigma_e \sim (n^2+2)^2/n$) [18] and inversely proportional to the half-width of the emission band. Moreover, it is apparent that $Er^{3+}$:RTFP glasses possess large stimulated emission cross-sections to utilize these glasses for broadband and high-gain amplification devices. A figure of merit (FOM) for the bandwidth is the product FWHM $\times \sigma_e$, which indicates the gain bandwidth of an amplifier. The $^4I_{13/2} \rightarrow {}^4I_{15/2}$ emission properties like FWHM, $\sigma_e$ and FOM of $Er^{3+}$ ions in different glass hosts [37–39] are shown in table 6 along with the refractive indices. Generally transitions with large stimulated emission cross-sections exhibit low threshold and high gain laser operation. From table 6, it can be realized that $Er^{3+}$:RTFP glasses are good host materials for broadband amplifiers and also for laser applications in the near-infrared region.

### *3.4. Luminescence decay*

The radiative decay from the $^4S_{3/2}$ level of $Er^{3+}$ ions in tellurofluorophosphate glasses is fitted with a nearly single exponential function as shown in figure 5. The lifetime ($\tau_{meas}$) of any

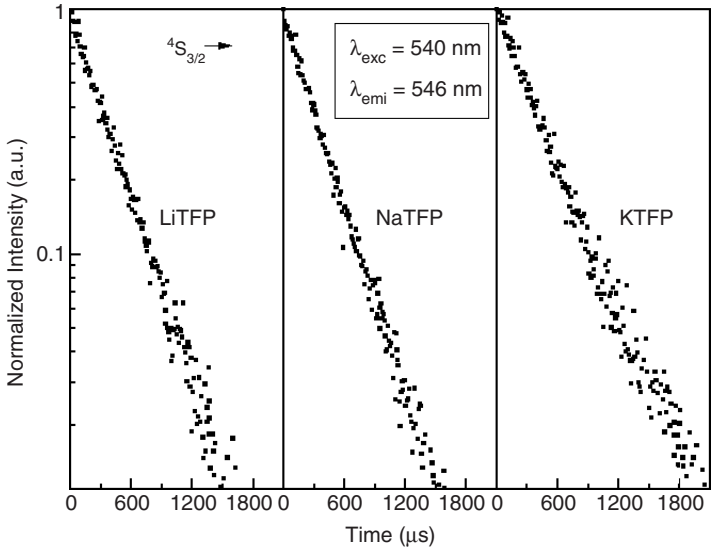


**Figure 5.** Luminescence decay profile of the $^4S_{3/2}$ level in $Er^{3+}$:RTFP glasses.

**Table 6.** NIR emission parameters of the $^4I_{13/2} \rightarrow {}^4I_{15/2}$ transition for $Er^{3+}$ in various glass hosts.

| Glasses | Refractive index | FWHM | $\sigma_e$ ($\times 10^{-21}$ cm$^2$) | FOM ($\sigma_e \times$ FWHM) | Reference |
|---|---|---|---|---|---|
| LiTFP | 1.585 | 37.9 | 11.29 | 427.9 | This work |
| NaTFP | 1.586 | 39.3 | 11.70 | 459.8 | This work |
| KTFP | 1.582 | 36.4 | 12.42 | 452.1 | This work |
| Silicate | 1.585 | 40 | 5.50 | 220 | [37] |
| Phosphate | 1.569 | 37 | 6.40 | 236.8 | [38] |
| Germanate | 1.625 | 53 | 5.68 | 301 | [39] |

excited state is defined as the $1/e$ decay time of the fluorescence intensity. The measured lifetimes of the $^4S_{3/2}$ level in LiTFP, NaTFP and KTFP are 330, 314 and 403 $\mu$s, respectively. These values are comparable to those reported for $BaF_2$–$ThF_4$ (300 $\mu$s) [40], oxyfluoroborate (239 $\mu$s) [41] and fluorozirconate (398 $\mu$s) [42] glasses. The predicted radiative lifetimes for the $^4S_{3/2}$ level using JO theory are 575, 513 and 514 $\mu$s for LiTFP, NaTFP and KTFP respectively. From the measured and predicted radiative lifetimes, the quantum efficiency $\eta = \tau_{meas}/\tau_R$ for the transition $^4S_{3/2} \rightarrow {}^4I_{15/2}$ at 0.5 $\mu$m of $Er^{3+}$:RTFP glasses are found to be approximately 57%, 61% and 78% respectively. The non-radiative relaxation rate ($W_{NR} = 1/\tau_{meas} - 1/\tau_R$) for $Er^{3+}$-doped LiTFP, NaTFP and KTFP obtained are 1291, 1235 and 536 s$^{-1}$, respectively. The luminescence decay properties such as lifetimes, quantum efficiencies, and non-radiative relaxation rates are given in table 7. However, we were not able to measure the decay times and in turn the quantum efficiencies for the emission transition $^4I_{13/2} \rightarrow {}^4I_{15/2}$ at 1534 nm due to the lack of experimental facilities in the near-infrared region.

## 4. Conclusion

Optical absorption, fluorescence and luminescence decay analyses of $Er^{3+}$-doped tellurofluorophosphate glasses have been performed. The Judd–Ofelt model has been applied

**Table 7.** Quantum efficiencies, lifetimes and non-radiative relaxation rates for the $^4S_{3/2}$ level of $Er^{3+}$:RTFP glasses.

| | | $\tau$ | | |
|---|---|---|---|---|
| Host | $\eta$ (%) | $\tau_{meas}$ ($\mu$s) | $\tau_{cal}$ ($\mu$s) | $W_{NR}$ ($s^{-1}$) |
| LiTFP | 57.4 | 330 | 575 | 1291 |
| NaTFP | 61.2 | 314 | 513 | 1235 |
| KTFP | 78.4 | 403 | 514 | 536 |

to calculate the JO intensity parameters from the measured oscillator strength of the absorption spectra of $Er^{3+}$:RTFP glasses. The spectroscopic quality factors ($X = \Omega_4/\Omega_6$), which are critically important in predicting the stimulated emission of any laser active medium, are determined. The spectroscopic quality factors for $Er^{3+}$ in LiTFP, NaTFP and KTFP are found to be 0.934, 0.743 and 0.477, which are higher than that of $Er^{3+}$:YAG (0.32) [28]. The line strength ratios ($S_{ed}/S_{ed} + S_{md}$) calculated for the $^4I_{13/2} \rightarrow {}^4I_{15/2}$ transition shows that these glasses possess larger gain bandwidth at 1.5 $\mu$m. The radiative lifetimes, spontaneous emission probabilities and branching ratios for all the excited $^4G_{11/2}$, $^2H_{9/2}$, $^4F_{5/2}$, $^4F_{7/2}$, $^2H_{11/2}$, $^4S_{3/2}$, $^4F_{9/2}$, $^4I_{9/2}$, $^4I_{11/2}$ and $^4I_{13/2}$ states are predicted theoretically. From the visible emission spectra, the emission cross-sections for the $^2H_{11/2} \rightarrow {}^4I_{15/2}$, $^4S_{3/2} \rightarrow {}^4I_{15/2}$, $^4F_{5/2} \rightarrow {}^4I_{13/2}$ and $^4F_{9/2} \rightarrow {}^4I_{15/2}$ transitions are reported. For the near-infrared emission transition at 1.5 $\mu$m, the emission parameters such as FWHM, $\sigma_e$, FOM are determined and compared with other hosts. Measured lifetimes and quantum efficiencies for the $^4S_{3/2}$ level in LiTFP, NaTFP and KTFP have been reported at room temperature. The results of these investigations indicate that $Er^{3+}$-doped tellurofluorophosphate glasses may be useful for the development of lasers and fibre amplifiers.

## Acknowledgments

One of the authors (LRM) would like to thank the University Grants Commission (UGC), Government of India, New Delhi for sanctioning the Major Research Project No. F.10-23/2003(SR) to carry out the present research work. MJ is also grateful to the UGC for financial support through a project fellowship in the above project.

## References

[1] Vermelho M V D, Gonveia-Neto A S, Amorim H T, Cassanjes F C, Ribeiro S J L and Messaddeq Y 2003 *J. Lumin.* **102/103** 755
[2] Voronoko Y K, Sobol A A, Karasik A Y, Eskov N A, Rabochkina P A and Ushakov S N 2002 *Opt. Mater.* **20** 197
[3] Lazaro J A, Valles J A and Rebolledo M A 1999 *IEEE. J. Quantum Electron.* **35** 827
[4] Cheng C 2004 *Opt. Laser Technol.* **36** 607
[5] Hattori K, Kitagawa T, Oguma M, Okazaki H and Ohmori Y 1996 *J. Appl. Phys.* **80** 5301
[6] Liu Z, Qi C, Dai S, Jiang Y and Hu L 2003 *Opt. Mater.* **21** 789
[7] Laporta P, Taccheo S, Longhi S, Svelto O and Svelto C 1999 *Opt. Mater.* **11** 269
[8] Jing H and Jianquan Y 2005 *Opt. Commun.* **251** 132
[9] Yeh C H, Lee C C and Chi S 2004 *Opt. Commun.* **241** 333
[10] Van Deun R, Nockemann P, Gorller-Walrand C and Binnemans K 2004 *Chem. Phys. Lett.* **397** 447
[11] Mierczyk Z, Kwasny M, Kopczynski K, Gietka A, Lukasiewicz T, Frukacz Z, Kisielewski J, Stepien R and Jedrzejewski K 2000 *J. Alloys Compounds* **300/301** 398
[12] Dragic P D 2005 *Opt. Commun.* **250** 403

[13] Hibst R 1992 *Lasers Surg. Med.* **12** 125
[14] Nagel D 1997 *Lasers Surg. Med.* **21** 79
[15] Ohishi Y, Mori A, Yamada M, Ono H, Nishida Y and Oikawa K 1998 *Opt. Lett.* **23** 274
[16] Atkins C G, Massicott J F, Armitage J P, Wyatt R, Ainslie B J and Craig-ryan S P 1989 *Electron. Lett.* **25** 910
[17] Mori A, Ohishi Y and Sudo S 1997 *Electron. Lett.* **33** 863
[18] Wang J S, Vogel E M and Snitzer E 1994 *Opt. Mater.* **3** 187
[19] Resfield R 1975 *Struct. Bonding* **22** 123
[20] Sidebottom D L, Green P F and Brow R K 1997 *J. Non-Cryst. Solids* **222** 354
[21] Judd B R 1962 *Phys. Rev.* **127** 750
[22] Ofelt G S 1962 *J. Chem. Phys.* **37** 511
[23] Vand Deun R, Binnemans K, Gorller-Walrand C and Adam J L 1999 *J. Alloys Compounds* **283** 59
[24] Rama Moorthy L, Srinivasa Rao T, Janardhnam K and Radhapathy A 2000 *Spectrochim. Acta* A **56** 1759
[25] Carnall W T, Crosswhite H and Crosswhite H M 1978 *Energy Level Structure and Transition Probabilities of Trivalent Lanthanides in* $LaF_3$ (Arogonne, IL: Argonne National Laboratories)
[26] Ravi Kanth Kumar V V, Jayasankar C K and Jagannathan R 1996 *Phys. Status Solidi* b **195** 287
[27] Sardar D K, Gruber J B, Zandi B, Hutchinson J A and Trussell C W 2003 *J. Appl. Phys.* **93** 2041
[28] Sardar D K, Bradley W M, Perez J J, Gruber J B, Zandi B, Hutchinson J A, Trussell C W and Kokta M R 2003 *J. Appl. Phys.* **93** 2602
[29] Lakshman S V J and Ratnakaram Y C 1987 *J. Non-Cryst. Solids* **94** 222
[30] Renuka Devi A and Jayasankar C K 1996 *J. Non-Cryst. Solids* **197** 111
[31] Weber M J 1982 *J. Non-Cryst. Solids* **47** 117
[32] Tanabe S 1999 *J. Non-Cryst. Solids* **259** 1
[33] Kaminskii A A 1981 *Laser Crystals* (Berlin: Springer)
[34] Pauling L 1929 *J. Am. Chem. Soc.* **51** 1010
[35] Porque J, Jiang S, Hwang B C, Fuflyigin V, Salley E, Zhao J and Peyghambarian N 2000 *Proc. SPIE* **3942** 60
[36] Pan Z, Morgam S H, Dyer K, Ueda A and Liu H 1996 *J. Appl. Phys.* **79** 8906
[37] Zou X and Izumitani T 1993 *J. Non-Cryst. Solids* **162** 68
[38] Jiang S, Luo T, Hwang B C, Smekatala F, Seneschal K, Lucas J and Peyghambarian N 2000 *J. Non-Cryst. Solids* **263/264** 364
[39] Lin H, Pun E Y B, Man S Q and Liu X R 2001 *J. Opt. Soc. Am.* B **18** 602
[40] Yeh D C, Pertin R R, Sibley W A, Madigou V, Adam J L and Suscavage M J 1989 *Phys. Rev.* B **39** 80
[41] Kumar A, Rai D K and Rai S B 2002 *Spectrochim. Acta* A **58** 3067
[42] Tsuda M, Soga K, Inoue H and Makishima A 2000 *J. Appl. Phys.* **88** 1900